Polyunsaturated phospholipids promote the oxidation and fragmentation of γ-hydroxyalkenals: formation and reactions of oxidatively truncated ether phospholipids[S]

Xi Chen,* Wujuan Zhang,* James Laird,* Stanley L. Hazen,[†,§,] and Robert G. Salomon[1,*]**

Department of Chemistry,* Case Western Reserve University, Cleveland, OH 44106; and Department of Cell Biology,[†] Department of Cardiovascular Medicine,[§] and Center for Cardiovascular Diagnostics and Prevention,** Cleveland Clinic, Cleveland, OH 44195

Abstract **Low density lipoprotein contains traces of biologically active platelet-activating factor (PAF)-like ether phosphatidylcholines (PCs). These oxidatively truncated alkylacylphosphatidylcholines (OxPAFs) are presumably formed through the oxidative truncation of 1-alkyl-2-polyunsaturated fatty acyl PCs. We now report that a diverse structural variety of OxPAFs are generated in small unilamellar vesicles (SUVs) upon myeloperoxidase (MPO)-promoted autoxidation of ether PCs that incorporate linoleoyl, arachidonyl, or docosahexaenoyl groups at the *sn*-2 position. Total syntheses are reported that confirm the identities of the new OxPAFs and will facilitate the evaluation of their biologically important chemistry and activities. Especially noteworthy is the formation of OxPAFs containing γ-hydroxyalkenal functionality. Analogous oxidatively truncated diacylphosphatidylcholines are biologically important because they and their more oxidized derivatives are strong ligands for the scavenger receptor CD36. Furthermore, their covalent adduction with proteins can interfere with protein function or generate biologically active carboxyalkylpyrrole derivatives. We now find a profound influence of membrane composition on the stability of OxPAFs. In the presence of a polyunsaturated diacyl PC, the linoleic acid ester of 2-lysophosphatidylcholine, MPO induces the oxidation of aldehydes to carboxylic acids and the further oxidative truncation of γ-hydroxyalkenals.** **Remarkably, these reactions do not occur readily with MPO in SUVs composed entirely of saturated diacyl-PCs. A mechanistic rationale is presented that can account for this dichotomy.**—Chen, X., W. Zhang, J. Laird, S. L. Hazen, and R. G. Salomon. **Polyunsaturated phospholipids promote the oxidation and fragmentation of γ-hydroxyalkenals: formation and reactions of oxidatively truncated ether phospholipids. *J. Lipid Res.* 2008.** 49: **832–846.**

Supplementary key words myeloperoxidase • platelet-activating factor • liquid chromatography-tandem mass spectrometry • low density lipoprotein

Manuscript received 25 June 2007 and in revised form 26 December 2007.

Published, JLR Papers in Press, December 29, 2007.
DOI 10.1194/jlr.M700598-JLR200

Oxidatively truncated phosphatidylcholines (PCs), which are generated through the autoxidation of polyunsaturated diacyl PCs, exhibit diverse and important biological activities. For example, atherosclerosis is a chronic inflammatory disease (1), and mounting evidence suggests that the oxidation of LDL plays a major role throughout the development and progression of the inflammatory process (2–5). LDL can be oxidatively modified to a form that can be recognized by macrophage scavenger receptors, which are expressed by each of the three major cell

Abbreviations: AA, arachidonic acid; A-PAF, 1-O-hexadecyl-2-azeleyl-sn-glycero-3-phosphatidylcholine; AA-PAF, 1-*O*-hexadecyl-2-arachidonoyl-*sn*-3-phosphatidylcholine; CEP, carboxyethylpyrrole; DHA, docosahexaenoic acid; DHA-PAF, 1-*O*-hexadecyl-2-docosahexaenoyl-*sn*-3-phosphatidylcholine; G-PAF, 1-*O*-hexadecyl-2-glutaroyl-*sn*-glycero-3-phosphatidylcholine; HDdiA-PAF, 1-*O*-hexadecyl-2-(11-carboxy-9-hydroxyundec-10-enoyl)-*sn*-glycero-3-phosphatidylcholine; HHdiA-PAF, 1-*O*-hexadecyl-2-(7-carboxy-4-hydroxyhex-5-enoyl)-*sn*-glycero-3-phosphatidylcholine; HODA-PAF, 1-*O*-hexadecyl-2-(9-hydroxy-12-oxododec-10-enoyl)-*sn*-glycero-3-phosphatidylcholine; HOdiA-PAF, 1-*O*-hexadecyl-2-(5-hydroxy-7-carboxyhept-6-enoyl)-*sn*-glycero-3-phosphatidylcholine; HOHA-PAF, 1-*O*-hexadecyl-2-(4-hydroxy-7-oxohept-5-enoyl)-*sn*-glycero-3-phosphatidylcholine; HOOA-PAF, 1-*O*-hexadecyl-2-(5-hydroxy-8-oxooct-6-enoyl)-*sn*-glycero-3-phosphatidylcholine; KDdiA-PAF, 1-*O*-hexadecyl-2-(11-carboxy-9-oxoundec-10-enoyl)-*sn*-glycero-3-phosphatidylcholine; KHdiA-PAF, 1-*O*-hexadecyl-2-(6-carboxy-4-oxohex-5-enoyl)-*sn*-glycero-3-phosphatidylcholine; KODA-PAF, 1-*O*-hexadecyl-2-(9-oxo-12-oxododec-10-enoyl)-*sn*-glycero-3-phosphatidylcholine; KOdiA-PAF, 1-*O*-hexadecyl-2-(7-carboxy-5-oxohep-6-enoyl)-*sn*-glycero-3-phosphatidylcholine; KOHA-PAF, 1-*O*-hexadecyl-2-(4-oxo-7-oxohept-5-enoyl)-*sn*-glycero-3-phosphatidylcholine; KOOA-PAF, 1-*O*-hexadecyl-2-(5-oxo-8-oxooct-6-enoyl)-*sn*-glycero-3-phosphatidylcholine; LA, linoleic acid; LA-PAF, 1-*O*-hexadecyl-2-linoleoyl-*sn*-glycero-3-phosphatidylcholine; LA-PC, linoleic acid ester of 2-lysophosphatidylcholine; lyso-PAF, 1-alkyl-2-hydroxy-*sn*-glycero-3-phosphocholine; MPO, myeloperoxidase; MRM, multiple reaction monitoring; OB-PAF, 1-*O*-hexadecyl-2-(4-oxobutyroyl)-*sn*-glycero-3-phosphatidylcholine; ON-PAF, 1-*O*-hexadecyl-2-(9-oxononanoyl)-*sn*-glycero-3-phosphatidylcholine; OV-PAF, 1-*O*-hexadecyl-2-(5-oxovaleroyl)-*sn*-glycero-3-phosphatidylcholine; OxLDL, oxidized low density lipoprotein; OxPAF, oxidatively truncated alkylacylphosphatidylcholine; OxPC, oxidatively truncated diacylphosphatidylcholine; PAF, platelet-activating factor; PAFR, platelet-activating factor receptor; PC, phosphatidylcholine; S-PAF, 1-*O*-hexadecyl-2-succinoyl-*sn*-glycero-3-phosphatidylcholine; SUV, small unilamellar vesicle.

[1] To whom correspondence should be addressed.
e-mail: rgs@case.edu

[S] The online version of this article (available at http://www.jlr.org) contains supplementary data.

types of the arterial wall: endothelial cells, smooth muscle cells, and macrophages (6). Several reports demonstrated the generation of a variety of oxidatively truncated diacylphosphatidylcholines (OxPCs) that mediate the atherogenic effects of oxidatively modified LDL (7–12). The phospholipids from oxidized low density lipoprotein (OxLDL) may also play a role in regulating vascular calcification (13) and the inflammatory functions of endothelial cells (14). Several lipid oxidation products derived from 1-palmitoyl-2-arachidonyl-*sn*-glycero-3-phosphocholine and 1-palmitoyl-2-linoleyl-*sn*-glycero-3-phosphocholine were shown to play a major role in the binding of OxLDL, but not native LDL, to the scavenger receptor CD36, triggering endocytosis by macrophages (15, 16). The highest affinity ligands are a family of OxPCs that contain γ-hydroxyalkenal functionality as well as ketoacids derived from them. These same OxPCs are also generated through the light-induced oxidation of photoreceptor rod outer segments in the retina, where they serve as ligands for the CD36-mediated phagocytosis of oxidatively damaged photoreceptors, a tissue with one of the highest turnover rates in the body, by retinal pigment epithelial cells (17).

OxPCs that contain γ-hydroxyalkenal functionality can interfere with the biological activities of proteins as a result of covalent adduction to the ε-amino groups of protein lysyl residues (18, 19) or thiol groups of cysteine residues (20). Most recently, it was found that the modification of proteins by a γ-hydroxyalkenal OxPC, the 4-hydroxy-7-oxo-5-heptenoate ester of 2-lysophosphatidylcholine (HOHA-PC), produces carboxyethylpyrroles (CEPs) that incorporate the ε-amino group of lysyl residues. CEPs accumulate in the retinas of individuals with age-related macular degeneration, where they promote choroidal neovascularization (21). They also promote angiogenesis in rat cornea (21).

Platelet-activating factor (PAF), structurally identified as 1-*O*-hexadecyl-2-acetyl-*sn*-glycero-3-phosphocholine, is an ether phospholipid with potent, diverse physiological actions, particularly as a mediator of inflammation (22). It exerts its effects through a single, highly specific G-protein-coupled serpentine receptor (23) that is expressed by all members of the innate immune system. The *sn*-1 ether bond, a short *sn*-2 residue (i.e., acetyl), and the choline head group of the PAF are crucial for its high-affinity recognition by the platelet-activating factor receptor (PAFR) (9). As the most potent phospholipid agonist yet identified, PAF's biosynthesis is closely controlled.

Unlike the highly regulated synthesis of the PAF, PAF-like phospholipids can be generated nonenzymatically under oxidative stress (24). The oxidative fragmentation of PUFA residues esterfied at the *sn*-2 position shortens this side chain. Some of these PAF-like oxidatively truncated alkylacylphosphatidylcholines (OxPAFs), which are generated during the oxidation of LDL, stimulate the proliferation of smooth muscle cells, and their effect is blocked by antagonists of the PAF receptor (8). Evidence for the presence of tiny amounts of OxPAF in OxLDL was obtained by mass spectroscopic comparison of synthetic butanoyl, butenoyl (9) and azeleyl (25) esters of 1-alkyl-2-hydroxy-*sn*-glycero-3-phosphocholine (lyso-PAF), with ether lipids isolated from OxLDL. Although the two C_4 analogs are 10-fold less potent than PAF as PAFR ligands and agonists, they are 100-fold more abundant than PAF in OxLDL.

Our previous studies identified families of OxPCs and oxidatively truncated diacylphosphatidylethanolamines that are generated through the oxidative fragmentation of linoleic acid (LA), arachidonic acid (AA), and docosahexaenoic acid (DHA) esters of 2-lysophosphatidylcholine (11, 16, 17, 26) and 2-lysophosphatidylethanolamine (27). By analogy, we predicted that OxPAFs **2–7** would be generated through the autoxidation of corresponding esters of lyso-PAF (**Fig. 1**). Treatment of the lipid mixture extracted from OxLDL with phospholipase A_1 removes diacyl phospholipids, leaving a biologically active fraction rich in ether phospholipids (25). The electrospray mass spectrum of this fraction exhibited many molecular ions of unknown structure that may correspond to some putative OxPAFs depicted in Fig. 1, such as ions with mass/charge ratios expected for 1-*O*-hexadecyl-2-glutaroyl-*sn*-glycero-3-phosphatidylcholine (G-PAF; *m/z* 596), 1-*O*-hexadecyl-2-(7-carboxy-5-oxohept-6-enoyl)-*sn*-glycero-3-phosphatidylcholine (KOdiA-PAF; *m/z* 652), 1-*O*-hexadecyl-2-(11-carboxy-9-oxoundec-10-enoyl)-*sn*-glycero-3-phosphatidylcholine (KDdiA-PAF; *m/z* 706), 1-*O*-hexadecyl-2-(9-oxo-12-oxododec-10-enoyl)-*sn*-glycero-3-phosphatidylcholine (KODA-PAF; *m/z* 690), and 1-*O*-hexadecyl-2-(5-oxo-8-oxooct-6-enoyl)-*sn*-glycero-3-phosphatidylcholine (KOOA-PAF; *m/z* 634) (25).

We now report that the entire family of oxidatively truncated ether phospholipids **2–7** is generated through oxidative cleavage of 2-lyso-PAF esters of LA, AA, and DHA in small unilamellar vesicles (SUVs) using the biologically relevant myeloperoxidase (MPO)/H_2O_2/NO_2^- system to initiate autoxidation. To confirm the identification and facilitate the quantification of these OxPAFs, we also prepared pure samples of the phospholipids **2–7** by unambiguous chemical syntheses. These pure samples will also be valuable for evaluating the biological activities of these OxPAFs that may contribute to the proatherogenic activity of OxLDL.

Some of these OxPAFs are stable end products of lipid autoxidation. Most interestingly, we discovered a profound influence of membrane composition on the stability of γ-hydroxyalkenal OxPAFs. Thus, in SUVs composed of a saturated PC, MPO-mediated oxidation of 1-*O*-hexadecyl-2-(4-hydroxy-7-oxohept-5-enoyl)-*sn*-glycero-3-phosphatidylcholine (HOHA-PAF) only generates the corresponding γ-ketoalkenal. In contrast, in SUVs that contain the polyunsaturated LA ester of 2-lysophosphatidylcholine, HOHA-PAF is not only oxidized to the corresponding γ-ketoalkenal but also into carboxylic acid analogs, and it is also oxidatively fragmented into shorter chain products. A mechanistic rationale will be presented that can account for this dichotomy.

MATERIALS AND METHODS

General methods

^{1}H NMR spectra were recorded on Varian Gemini spectrometers operating at 200 or 300 MHz and on a Varian Inova AS400 spectrometer operating at 400 MHz. Proton chemical shifts are

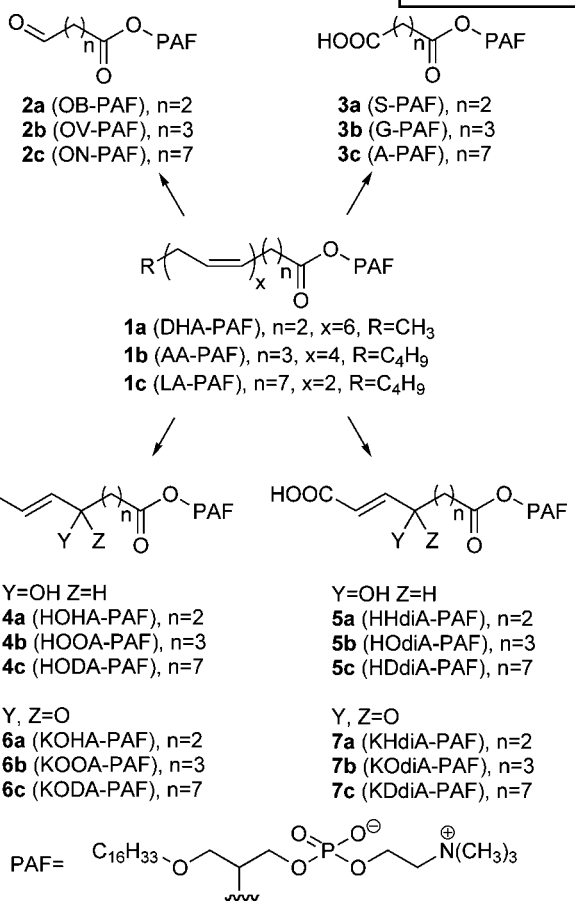

Fig. 1. Oxidatively truncated alkylacylphosphatidylcholines (OxPAFs) expected to be generated through the autoxidation of polyunsaturated esters of 2-1-alkyl-2-hydroxy-*sn*-glycero-3-phosphocholine (lyso-PAF). AA-PAF, 1-*O*-hexadecyl-2-arachidonoyl-*sn*-3-phosphatidylcholine; A-PAF, 1-*O*-hexadecyl-2-azeleyl-*sn*-glycero-3-phosphatidylcholine; DHA-PAF, 1-*O*-hexadecyl-2-docosahexaenoyl-*sn*-3-phosphatidylcholine; G-PAF, 1-*O*-hexadecyl-2-glutaroyl-*sn*-glycero-3-phosphatidylcholine; HDdiA-PAF, 1-*O*-hexadecyl-2-(11-carboxy-9-hydroxyundec-10-enoyl)-*sn*-glycero-3-phosphatidylcholine; HHdiA-PAF, 1-*O*-hexadecyl-2-(6-carboxy-4-hydroxyhex-5-enoyl)-*sn*-glycero-3-phosphatidylcholine; HODA-PAF, 1-*O*-hexadecyl-2-(9-hydroxy-12-oxododec-10-enoyl)-*sn*-glycero-3-phosphatidylcholine; HOdiA-PAF, 1-*O*-hexadecyl-2-(7-carboxy-5-hydroxyhep-6-enoyl)-*sn*-glycero-3-phosphatidylcholine; HOHA-PAF, 1-*O*-hexadecyl-2-(4-hydroxy-7-oxohept-5-enoyl)-*sn*-glycero-3-phosphatidylcholine; HOOA-PAF, 1-*O*-hexadecyl-2-(5-hydroxy-8-oxooct-6-enoyl)-*sn*-glycero-3-phosphatidylcholine; KDdiA-PAF, 1-*O*-hexadecyl-2-(11-carboxy-9-oxoundec-10-enoyl)-*sn*-glycero-3-phosphatidylcholine; KHdiA-PAF, 1-*O*-hexadecyl-2-(6-carboxy-4-oxohex-5-enoyl)-*sn*-glycero-3-phosphatidylcholine; KODA-PAF, 1-*O*-hexadecyl-2-(9-oxo-12-oxododec-10-enoyl)-*sn*-glycero-3-phosphatidylcholine; KOdiA-PAF, 1-*O*-hexadecyl-2-(7-carboxy-5-oxohept-6-enoyl)-*sn*-glycero-3-phosphatidylcholine; KOHA-PAF, 1-*O*-hexadecyl-2-(4-oxo-7-oxohept-5-enoyl)-*sn*-glycero-3-phosphatidylcholine; KOOA-PAF, 1-*O*-hexadecyl-2-(5-oxo-8-oxooct-6-enoyl)-*sn*-glycero-3-phosphatidylcholine; LA-PAF, 1-*O*-hexadecyl-2-linoleoyl-*sn*-glycero-3-phosphatidylcholine; OB-PAF, 1-*O*-hexadecyl-2-(4-oxobutyroyl)-*sn*-glycero-3-phosphatidylcholine; ON-PAF, 1-*O*-hexadecyl-2-(9-oxononanoyl)-*sn*-glycero-3-phosphatidylcholine; OV-PAF, 1-*O*-hexadecyl-2-(5-oxovaleroyl)-*sn*-glycero-3-phosphatidylcholine; S-PAF, 1-*O*-hexadecyl-2-succinoyl-*sn*-glycero-3-phosphatidylcholine.

reported in ppm on the δ scale relative to $CDCl_3$ (δ 7.24) or CD_3OD (δ 3.30). ^{13}C NMR spectra were recorded on a Varian Gemini spectrometer operating at 50 MHz or on a Varian Inova AS400 spectrometer operating at 100 MHz. All high-resolution mass spectra were recorded on a Kratos AEI MS25 RFA high-resolution mass spectrometer at 20 eV. Thin-layer chromatography was performed on glass plates precoated with silica gel (Kieselgel 60 F_{254}; E. Merck, Darmstadt, Germany). Rf values are quoted for plates of thickness 0.25 mm. The plates were visualized by viewing under short-wavelength ultraviolet light or by exposure to iodine vapor. Flash column chromatography was performed using Silica Gel 60A, 32–63 μm, from Sorbent Technologies (Atlanta, GA) or ICN SiliTech 60A from ICN Biomedicals GmbH (Eschwege, Germany). HPLC was performed with a Waters 600 solvent delivery system (Waters, Wilmington, DE) coupled with a 2996 photodiode array detector, a SEDEX 75 evaporative light-scattering detector, and a Waters 717 autosampler. A Luna 5μ C18 (2) column (250 × 10 mm or 250 × 4.6 mm; Phenomenex, Torrance, CA) was used for reverse-phase HPLC separation. All phospholipids were obtained from Avanti Polar Lipids, Inc. (Alabaster, AL), and all other chemicals were obtained from Aldrich (Milwaukee, WI) or Fisher Scientific (Pittsburgh, PA). For all reactions performed in an inert atmosphere, argon was used unless specified otherwise.

Lipid oxidation in SUVs

SUVs were prepared from hydrated lipids as described elsewhere (16, 28). Briefly, 10 mol% of specific native phospholipid, 1-*O*-hexadecyl-2-docosahexaenoyl-*sn*-glycero-3-phosphatidylcholine (DHA-PAF), 1-*O*-hexadecyl-2-arachidonoyl-*sn*-glycero-3-phosphatidylcholine (AA-PAF), 1-*O*-hexadecyl-2-linoleoyl-*sn*-glycero-3-phosphatidylcholine (LA-PAF), HOHA-PAF, or HOHA-PAF/linoleic acid ester of 2-lysophosphatidylcholine (LA-PC) (1:1), in freshly distilled chloroform with 1,2-dinonadecanoyl-*sn*-glcero-3-phosphocholine as lipid carrier, was freed of solvent by evaporation under a stream of dry nitrogen. SUVs were prepared in argon-sparged sodium phosphate buffer (50 mM; pH 7.0) supplemented with 100 μM diethylenetriamine pentaacetic acid by extrusion (20 times) through a 0.1 μm polycarbonate filter using an Avanti Mini-Extruder (Avanti Polar Lipids). The vesicles (0.1 mg total lipids/ml) were incubated in the presence of MPO (30 nM), glucose oxidase (100 ng/ml), glucose (100 μg/ml), and $NaNO_2$ (500 μM) in sodium phosphate buffer (50 mM) with diethylenetriamine pentaacetic acid (200 μM) at 37°C. The reaction was stopped by adding butylated hydroxytoluene (40 μM) and catalase (150 μM). The lipids were extracted by the method of Bligh and Dyer (29), and the samples were freed of solvent by evaporation under a stream of dry nitrogen and stored in vials sealed under argon at −80°C.

Chemical synthesis of OxPAFs

Experimental details for the preparation, ^1H and ^{13}C NMR, and mass spectroscopic characterization of the OxPAFs **2–7** and precursors **8–12** are provided in the supplementary data.

LC-MS analysis of phospholipids

LC-MS analyses of the phospholipids were performed on a Quattro Ultima mass spectrometer (Micromass, Wythenshawe, UK) equipped with an ESI probe interfaced with a Waters Alliance 2690 HPLC system. The phospholipid samples were dissolved in methanol (200–250 μl), and the resulting solution (50 μl) was chromatographed on a Prodigy ODS C18 column (150 × 2 mm, 5 μm; Phenomenex) with a binary solvent gradient, starting from 85% methanol in water. A linear gradient

was run from 85% methanol to 88% methanol in water over 10 min, and then over 2 min the mobile phase was linearly changed to 100% methanol at a flow rate of 0.2 ml/min. After holding this solvent composition for 25 min, the mobile phase was linearly changed back to the initial mobile phase composition (85% methanol in water) over 0.5 min, and the column was equilibrated under this condition for at least 7 min before the next injection. All of the mobile phase solvent contained 0.2% formic acid to enhance the MS signal. The total ion current was measured in the mass range of *m/z* 200–1,000 at 30 V of cone energy in the positive ion mode. Three kilovolts was applied to the electrospray capillary.

Derivatization of oxidized phospholipids

Methoxime derivatives of lipids were prepared by incubating the lipid (20–50 μg) in freshly dried pyridine containing 10% methoxylamine hydrochloride (200 μl) overnight at room temperature. Pentafluorobenzyl ester derivatives of lipids were prepared by suspending dried samples (20–50 μg) in freshly dried acetonitrile containing 10% pentafluorobenzyl bromide and 20% *N,N*-diisopropylethylamine (500 μl) at room temperature for 1 h. Solvent and volatile byproducts were removed under a stream of nitrogen. The product mixture was dissolved in 50% methanol in water. Nonlipid components were removed by passage over a C18 minicolumn (Strata C18-T SPE tubes, 6 ml; Phenomenex) by eluting with 75% methanol in water (6 ml). The lipid derivatives were then eluted with methanol (2 ml), and the solvents were evaporated with a stream of dry nitrogen. Derivatives were then dissolved in methanol (200 μl), and 50 μl of the solution was injected into the LC-MS system. They were characterized with ESI-MS/MS and chromatography on a Prodigy ODS C18 column (150 × 2 mm, 5 μm; Phenomenex). The eluate was introduced into an LC-MS/MS system operated in the positive ion mode. The analytes were detected by multiple reaction monitoring (MRM).

Microphosphorus assay

The concentrations of synthetic lipid solutions were calibrated with a standard microphosphorus assay (30) that was modified to measure phospholipids at the level of 10–20 μg. Lipid (15–25 μg) was digested in perchloric acid (0.2 ml of 72% aqueous solution) in a glass 5 ml disposable cell culture tube that was heated to boiling in a sand bath. A yellow color appeared and then disappeared during the process. Then, water (2.1 ml), aqueous ammonium molybdate (0.1 ml of 5% aqueous solution), and aqueous amidol reagent (0.1 ml) containing 1% amidol (2,4-diaminophenol dihydrochloride) and 20% sodium bisulfite were sequentially added to the tube, which was vortexed. The tube was covered with a beaker and heated in a boiling-water bath for 7 min. Then, the tube was cooled and the absorbance of the stable blue color was measured with an ultraviolet/visible light spectrometer at 830 nm in a 1 cm cuvette after 15 min. A standard calibration curve was obtained using 0, 0.5, 1, 2, and 4 μg of P obtained from a stock solution of KH_2PO_4 (40 μg P/ml).

RESULTS AND DISCUSSION

Synthesis of OxPAFs

Of the PAF analogs expected to be generated by oxidative cleavage of DHA, AA, and LA esters **1a–c** of lyso-PAF (Fig. 1), 1-O-hexadecyl-2-azeleyl-sn-glycero-3-phosphatidylcholine (A-PAF) (**3c**) was identified previously in OxLDL and shown to serve as a specific high-affinity ligand and agonist for peroxisome proliferator-activated receptor γ (25). Owing to their relatively short *sn*-2 residues, **2a–b** and **3a–b** are potential ligands for the PAFR. Chemical syntheses, outlined in **Fig. 2**, were developed to provide pure samples of the PAF analogs **2a–c** and **3a–c**. Coupling of the lyso-PAF with the appropriate commercially available alkenoic acids gave the alkenoylphospholipids **8a–c**. Subsequent ozonolyses delivered the desired aldehydes, 1-*O*-hexadecyl-2-(4-oxobutyroyl)-*sn*-glycero-3-phosphatidylcholine (OB-PAF; **2a**), 1-*O*-hexadecyl-2-(5-oxovaleroyl)-*sn*-glycero-3-phosphatidylcholine (OV-PAF; **2b**), or 1-*O*-hexadecyl-2-(9-oxononanoyl)-*sn*-glycero-3-phosphatidylcholine (ON-PAF; **2c**). Esterification of 2-lyso-PAF with succinic or glutaric anhydride delivered 1-*O*-hexadecyl-2-succinoyl-*sn*-glycero-3-phosphatidylcholine (S-PAF; **3a**) or glutaryl-PAF (G-PAF; **3b**). Azeleyl-PAF (**3c**) was prepared from ON-PAF (**2c**) by oxidation of the aldehyde functional group.

The 2-lyso-PAF esters of 4-hydroxy-7-oxohept-5-enoic acid (HOHA-PAF; **4a**), 1-*O*-hexadecyl-2-(5-hydroxy-8-oxooct-6-enoyl)-*sn*-glycero-3-phosphatidylcholine (HOOA-PAF; **4b**), and 1-*O*-hexadecyl-2-(9-hydroxy-12-oxododec-10-enoyl)-*sn*-glycero-3-phosphatidylcholine (HODA-PAF; **4c**) were expected to be chemically unstable (vide infra). Therefore, a strategy was devised, outlined in **Fig. 3**, to generate them from chemically more stable precursors that could be safely stored until needed. Acids **9a–c**, which contain the carbon skeletons of the desired HOHA, HOOA, and HODA with a 3,3-dimethyl-2, 4-dioxolanyl moiety as a latent aldehyde, were prepared as described previously (26, 31). Esterification of acids **9a–c** with 2-lyso-PAF provided the chemically stable precursors **10a–c**. The target aldehydes **4a–c** can be generated as needed by the hydrolysis

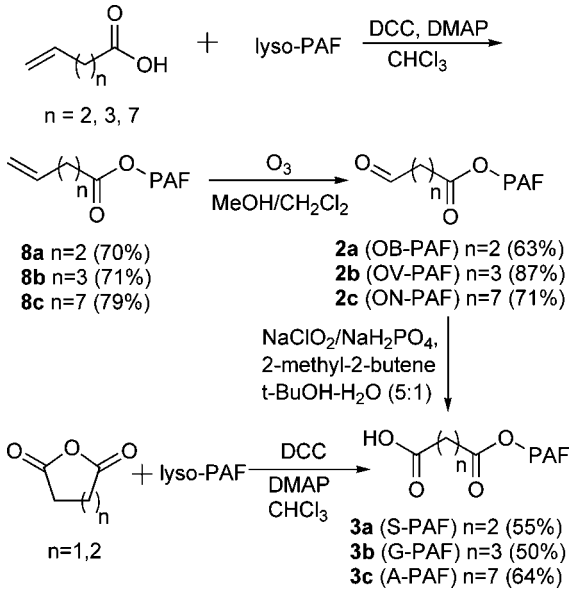

Fig.2. Chemical syntheses of OB-, OV-, ON-, S-, G-, and A-PAFs. DCC, dicyclohexylcarbodiimide; DMAP, 4-(N,N-dimethylamino)pyridine.

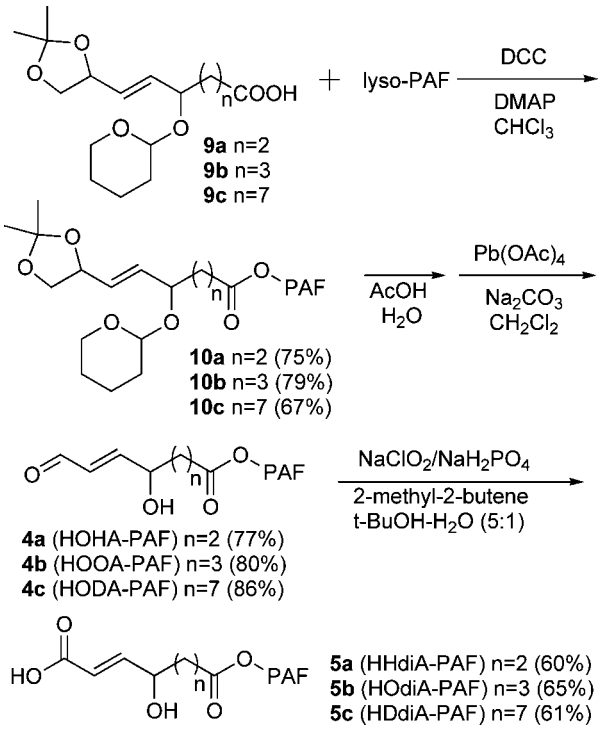

Fig. 3. Chemical syntheses of HOHA-, HOOA-, HODA-, HHdiA-, HOdiA-, and HDdiA-PAFs.

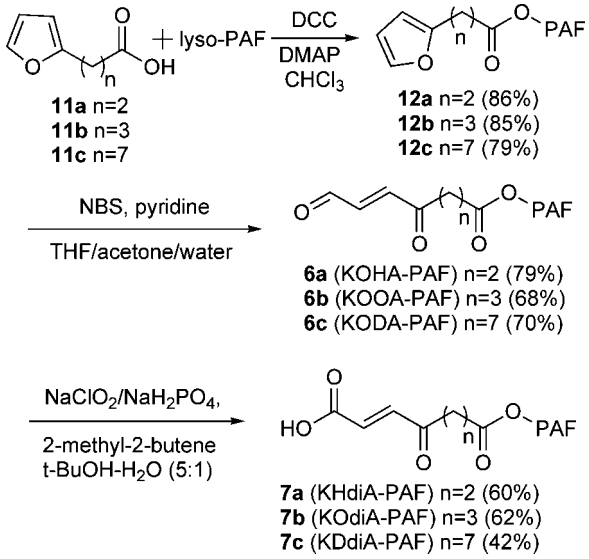

Fig. 4. Chemical syntheses of KOHA-, KOOA-, KODA-, KHdiA-, KOdiA-, and KDdiA-PAFs. NBS, *N*-bromosuccinimide; THF, tetrahydrofuran.

of **10a–c** in acetic acid, followed by oxidative cleavage of the resulting vicinal diol intermediate with lead tetraacetate at −78°C. The α,β-unsaturated dicarboxylic acid monoesters of 2-lyso-PAF, 1-*O*-hexadecyl-2-(6-carboxy-4-hydroxyhex-5-enoyl)-*sn*-glycero-3-phosphatidylcholine (HHdiA-PAF; **5a**), 1-*O*-hexadecyl-2-(7-carboxy-5-hydroxyhept-6-enoyl)-*sn*-glycero-3-phosphatidylcholine (HOdiA-PAF; **5b**), and 1-*O*-hexadecyl-2-(11-carboxy-5-hydroxyundec-10-enoyl)-*sn*-glycero-3-phosphatidylcholine (HDdiA-PAF; **5c**), were obtained by the further selective oxidation of the correspond aldehydes with sodium chlorite in the presence of 2-methyl-2-butene and NaH_2PO_4 in *tert*-butyl alcohol and water (5:1, v/v).

The ω-(2-furyl)alkanoate esters (**12a–c**) of 2-lyso-PAF were prepared, as shown in **Fig. 4**, from the commercially available 3-furan-2-ylpropionic acid (**11a**) or the homologous furancarboxylic acids **11b** and **11c**, which were prepared as reported previously (32). The desired ketoalkenal OxPAFs 1-*O*-hexadecyl-2-(4-oxo-7-oxohept-5-enoyl)-*sn*-glycero-3-phosphatidylcholine (KOHA-PAF; **6a**), KOOA-PAF (**6b**), and KODA-PAF (**6c**) were generated from **12a–c** through *N*-bromosuccinamide-promoted oxidative ring opening of the furans without oxidation of the sensitive aldehyde group (Fig. 4). The corresponding keto acid OxPAFs 1-*O*-hexadecyl-2-(6-carboxy-4-oxohex-5-enoyl)-*sn*-glycero-3-phosphatidylcholine (KHdiA-PAF; **7a**), KOdiA-PAF (**7b**), and KDdiA-PAF (**7c**) were then prepared from the corresponding aldehyde phospholipids (**6a–c**), respectively, by selective oxidation of the aldehyde functional group.

Generation of OxPAFs from DHA-PAF, AA-PAF, and LA-PAF

Detecting the generation of oxidatively truncated phospholipids in LDL is complicated by the proclivity of some of them to form covalent adducts with proteins (vide infra). To preclude the sequestration of some OxPAFs through covalent adduction with the LDL protein apolipoprotein B, we monitored the oxidative cleavage of polyunsaturated ether phospholipids in a protein-free model system, SUVs, using the physiologically relevant MPO/H_2O_2/NO_2^- system to foster autoxidation. Several reports had suggested that reactive nitrogen intermediates can be generated from NO_2^- by the MPO/H_2O_2 system (33, 34). In this study, D-glucose/glucose oxidase was used to continuously generate H_2O_2 in situ. $NO_2^{\bullet}$ is the most likely intermediate product, and the regeneration of NO_2^- during the oxidation of substrates by $NO_2^{\bullet}$ makes it act as a catalyst in the oxidation of other substrates by MPO/H_2O_2 (35). To test the hypothesis that compounds **2–7** are generated during the oxidation of corresponding PUFA esters of lyso-PAF (DHA-PAF, AA-PAF, and LA-PAF), SUVs were exposed to air in the presence of the MPO/H_2O_2/NO_2^- system. Levels of the parent polyunsaturated PUFA esters of 2-lyso-PAF (DHA-PAF, AA-PAF, and LA-PAF) decreased continually upon exposure to the MPO/H_2O_2/NO_2^- system (**Fig. 5A**). In control experiments, levels of DHA-PAF, AA-PAF, and LA-PAF in vesicles exposed to air in buffer in the absence of MPO did not decrease (Fig. 5A). Levels of the anticipated oxidatively truncated lipids **2–7** detected during the autoxidations are shown in Fig. 5B–D. The identities of these OxPAFs were confirmed by comparisons with the corresponding pure lipids available through the chemical syntheses described above. Under similar conditions, but in the absence of MPO, little or no oxidation products were detectable (data not shown).

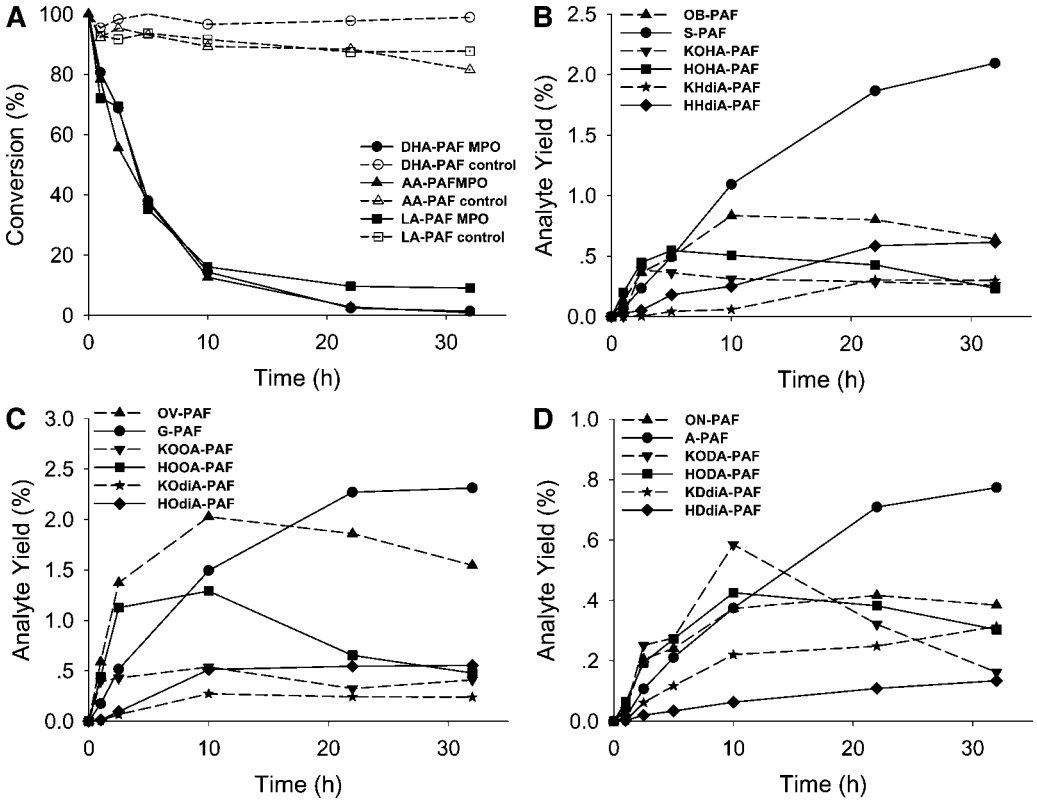

Fig. 5. Evolution profiles of the consumption of DHA-PAF, AA-PAF, and LA-PAF at various conditions (A), OxPAFs generated by the autoxidation of DHA-PAF (B), OxPAFs generated by the autoxidation of AA-PAF (C), and OxPAFs generated by the autoxidation of LA-PAF (D). Data are averages of two sets of independent experiments. MPO, myeloperoxidase.

Figure 5A, B and **Table 1** show the time course and maximum and final yields of OxPAFs produced through the MPO-promoted autoxidation of DHA-PAF. After incubation at 37°C for 32 h, 99% of DHA-PAF was consumed. Without MPO, the consumption of DHA-PAF was much slower, only 1% after 32 h. A stable end product, S-PAF, accumulated throughout the autoxidation reactions and was the most abundant species at long reaction times. The content of OB-PAF reached a maximum of 1.04% yield based on DHA-PAF in 10 h and then decreased to 0.80% yield by 32 h. Thus, OB-PAF is not a stable end product, and apparently it is further oxidized to S-PAF, whose yield reached 2.6% after 32 h. The yield of KOHA-PAF increased to 0.48% after 2.5 h but eventually declined to 0.32% after 32 h, apparently owing to further oxidation, which generates a more stable product, KHdiA-PAF. Likewise, the yield of HOHA-PAF reached 0.68% and then declined to 0.29% by 32 h. It should be noted that the levels of the γ-hydroxyalkenal HOHA-PAF exhibited the greatest decrease from its maximum of all the OxPAF generated from DHA-PAF. Further oxidation to KHdiA-PAF or HHdiA-PAF no doubt contributes to the eventual decline in levels of HOHA-PAF. The final yields of KHdiA-PAF and HHdiA-PAF were 0.37% and 0.76%, respectively. The oxidatively truncated phospholipids OB-PAF, S-PAF, KOHA-PAF, HOHA-PAF, KHdiA-PAF, and HHdiA-PAF accounted for 5.1% the DHA-PAF consumed in the MPO-initiated oxidation reaction.

Figure 5A, C and **Table 2** show the time course and the maximum and final yields for OxPAFs produced through MPO-promoted autoxidation of AA-PAF. In analogy with the autoxidation of DHA-PAF, 99% of AA-PAF

TABLE 1. Observed maximum and final amounts of OxPAFs and DHA-PAF

	Maximum		Final	
Phospholipids	Amount *pmol*	Yield %	Amount *pmol*	Yield %
DHA-PAF	15.0×10^3	100	201.2	1.34
OB-PAF	155.5	1.04	119.4	0.80
S-PAF	390.2	2.60	390.2	2.60
KOHA-PAF	67.5	0.48	48.2	0.32
HOHA-PAF	101.9	0.68	43.6	0.29
KHdiA-PAF	56.4	0.38	55.6	0.37
HHdiA-PAF	114.4	0.76	114.4	0.76

DHA-PAF, 1-*O*-hexadecyl-2-docosahexaenoyl-*sn*-3-phosphatidylcholine; HHdiA-PAF, 1-*O*-hexadecyl-2-(6-carboxy-4-hydroxyhex-5-enoyl)-*sn*-glycero-3-phosphatidylcholine; HOHA-PAF, 1-*O*-hexadecyl-2-(4-hydroxy-7-oxohept-5-enoyl)-*sn*-glycero-3-phosphatidylcholine; KHdiA-PAF, 1-*O*-hexadecyl-2-(6-carboxy-4-oxohex-5-enoyl)-*sn*-glycero-3-phosphatidylcholine; KOHA-PAF, 1-*O*-hexadecyl-2-(4-oxo-7-oxohept-5-enoyl)-*sn*-glycero-3-phosphatidylcholine; OB-PAF, 1-*O*-hexadecyl-2-(4-oxobutyroyl)-*sn*-glycero-3-phosphatidylcholine; OxPAF, oxidatively truncated alkylacylphosphatidylcholine; S-PAF, 1-*O*-hexadecyl-2-succinoyl-*sn*-glycero-3-phosphatidylcholine. Each value is the average of two independent studies (n = 2), starting with DHA-PAF (15 nmol).

TABLE 2. Observed maximum and final amounts of OxPAFs and AA-PAF

	Maximum		Final	
Phospholipids	Amount *pmol*	Yield %	Amount *pmol*	Yield %
AA-PAF	15.0×10^3	100	129.9	0.87
OV-PAF	274.6	1.83	209.4	1.40
G-PAF	313.2	2.09	13.2	2.09
KOOA-PAF	72.8	0.48	55.6	0.37
HOOA-PAF	152.7	1.17	64.7	0.43
KOdiA-PAF	36.9	0.25	32.5	0.22
HOdiA-PAF	74.9	0.50	74.9	0.50

AA-PAF, 1-*O*-hexadecyl-2-arachidonoyl-*sn*-3-phosphatidylcholine; G-PAF, 1-*O*-hexadecyl-2-glutaroyl-sn-glycero-3-phosphatidylcholine; HOdiA-PAF, 1-*O*-hexadecyl-2-(7-carboxy-5-hydroxyhept-6-enoyl)-sn-glycero-3-phosphatidylcholine; HOOA-PAF, 1-*O*-hexadecyl-2-(5-hydroxy-8-oxooct-6-enoyl)-sn-glycero-3-phosphatidylcholine; KOdiA-PAF, 1-*O*-hexadecyl-2-(7-carboxy-5-oxohept-6-enoyl)-sn-glycero-3-phosphatidylcholine; KOOA-PAF, 1-*O*-hexadecyl-2-(5-oxo-8-oxooct-6-enoyl)-sn-glycero-3-phosphatidylcholine; OV-PAF, 1-*O*-hexadecyl-2-(5-oxovaleroyl)-sn-glycero-3-phosphatidylcholine. Each value is the average of two independent studies (n = 2), starting with AA-PAF (15 nmol).

TABLE 3. Observed maximum and final amounts of OxPAFs and LA-PAF

	Maximum		Final	
Phospholipids	Amount *pmol*	Yield %	Amount *pmol*	Yield %
LA-PAF	15.0×10^3	100	1.35	9.01
ON-PAF	109.7	0.73	101.3	0.68
A-PAF	203.9	1.36	203.9	1.36
KODA-PAF	154.2	1.03	42.7	0.28
HODA-PAF	112.2	0.75	79.9	0.53
KDdiA-PAF	82.7	0.55	82.7	0.55
KHdiA-PAF	35.4	0.24	35.4	0.24

A-PAF, 1-*O*-hexadecyl-2-azeleoyl-sn-glycero-3-phosphatidylcholine; HDdiA-PAF, 1-*O*-hexadecyl-2-(11-carboxy-9-hydroxyundec-10-enoyl)-sn-glycero-3-phosphatidylcholine; HODA-PAF, 1-*O*-hexadecyl-2-(9-hydroxy-12-oxododec-10-enoyl)-sn-glycero-3-phosphatidylcholine; KDdiA-PAF, 1-*O*-hexadecyl-2-(11-carboxy-9-oxododec-10-enoyl)-sn-glycero-3-phosphatidylcholine; KDdia-PAF, 1-*O*-hexadecyl-2-(6-carboxy-4-oxohex-5-enoyl)-sn-glycero-3-phosphatidylcholine; KODA-PAF, 1-*O*-hexadecyl-2-(9-oxo-12-oxododec-10-enoyl)-sn-glycero-3-phosphatidylcholine; LA-PAF, 1-*O*-hexadecyl-2-linoleoyl-*sn*-glycero-3-phosphatidylcholine; ON-PAF, 1-*O*-hexadecyl-2-(9-oxononanoyl)-*sn*-glycero-3-phosphatidylcholine. Each value is the average of two independent studies (n = 2), starting with LA-PAF (15 nmol).

was consumed after 32 h of incubation. G-PAF accumulated throughout the autoxidation reaction and was the most abundant species at long reaction times. Thus, G-PAF is a stable end product from AA-PAF, analogous to S-PAF from DHA-PAF. By comparing the yields of homologous products in Tables 1, 2, we found that the maximum and final yields of OV-PAF were higher than those for OB-PAF, but the maximum and final yields of the G-PAF were lower than those for S-PAF. A similar trend was found in our previous study of the production of the oxidatively truncated diacyl phosphatidylethanolamines 1-palmityl-2-(4-oxobutyryl)-*sn*-glycero-3-phosphatidylethanolamine, 1-palmityl-2-(5-oxovaleryl)-*sn*-glycero-3-phosphatidylethanolamine, 1-palmityl-2-succinyl-*sn*-glycero-3-phosphatidylethanolamine, and 1-palmityl-2-glutaryl-*sn*-glycero-3-phosphatidylethanolamine from 1-palmityl-2-docosahexanoyl-*sn*-glycero-3-phosphatidylethanolamine or 1-palmityl-2-arachidonyl-*sn*-glycero-3-phosphatidylethanolamine under such oxidation conditions (27). KOOA-PAF, HOOA-PAF, and KOdiA-PAF reached their maximum levels after 10 h (0.48, 1.17, and 0.25% yield, respectively) and then decreased, eventually reaching 0.37, 0.43, and 0.22% yield after 32 h. It should be noted that the levels of the γ-hydroxyalkenal HOOA-PAF exhibited the greatest decrease from its maximum of all the OxPAF generated from AA-PAF. This is analogous to the variations observed in the levels of HOHA-PAF during the autoxidation of DHA-PAF (vide supra). Further oxidation to KOdiA-PAF or HOdiA-PAF no doubt contributes to the eventual decline in levels of HOOA-PAF. HOdiA-PAF levels increased continuously during the oxidation, and its yield reached 0.50% after 32 h. The total yield of the OxPAFs OV-PAF, G-PAF, KOOA-PAF, HOOA-PAF, KOdiA-PAF, and HOdiA-PAF accounted for 5.0% of the AA-PAF consumed in the MPO-initiated oxidation reaction.

Figure 5A, D and **Table 3** show the time course and the maximum and final yields of OxPAFs produced from MPO-promoted autoxidation of LA-PAF. Unlike the autoxidation of DHA-PAF and AA-PAF, the reaction did not go to completion in 32 h. Only 91% LA-PAF was consumed. A-PAF accumulated throughout the autoxidation reaction and is the most abundant species at long reaction times. A-PAF is a stable end product from LA-PAF, in analogy with the production of S-PAF from DHA-PAF and G-PAF from AA-APF. Both maximum and final yields of ON-PAF and A-PAF from LA-PAF were lower than those of OB-PAF and S-PAF from DHA-PAF or of OV-PAF and G-PAF from AA-PAF. There was also a notable difference between the levels of KODA-PAF generated in the autoxidation of LA-PAF and those of the analogs KOHA-PAF and KOOA-PAF generated in the autoxidation of DHA-PAF or AA-PAF. The maximum yield of KODA-PAF was ~2-fold greater than those of KOHA-PAF and KOOA-PAF. After prolonged reaction, however, the final yields of KOHA-PAF, KOOA-PAF, and KODA-PAF were similar: 0.32, 0.37, and 0.28%, respectively. Another important contrast in the product profile from LA-PAF (Fig. 5D) and those from DHA-PAF or AA-PAF (Fig. 5B, C) is that the fragmentation of LA-PAF produced more of the γ-ketoalkenal KDdiA-PAF than γ-hydroxyalkenal HDdiA-PAF. In the autoxidations of DHA-PAF and AA-PAF, more of the γ-hydroxyalkenals HHdiA-PAF and HOdiA-PAF were generated compared with the γ-ketoalkenals KHdiA-PAF and KOdiA-PAF, respectively. This may be because HDdiA-PAF is relatively more susceptible to further oxidative transformations (e.g., to produce KDdiA-PAF). We did observe that after 32 h, the yield of KDdiA-PAF (0.55%) was higher than that of its two analogs KHdiA-PAF and KOdiA-PAF (0.37% and 0.22%, respectively). But this could also be because, in the LA-PAF oxidation, there is a relatively higher yield of the γ-ketoalkenal KODA-PAF, which is oxidized further to KDdiA-PAF. The total yield of the OxPAFs ON-PAF, A-PAF, KOOA-PAF, HOOA-PAF, KOdiA-PAF, and HOdiA-PAF in these lipid fragments accounted for 3.64% of LA-PAF in the MPO-initiated oxidation.

Structure confirmation through derivatization of OxPAFs

To further verify the structures of the oxidatively truncated phospholipids, the oxidation product mixtures from DHA-PAF, AA-PAF, and LA-PAF were treated with methoxylamine hydrochloride or a mixture of pentafluorobenzyl bromide and diisopropylethylamine to derivatize aldehyde or ketone and carboxylic acid functionality. Methoxime derivatization of a single aldehyde or a ketone carbonyl results in a net increase of 29 Da, whereas pentafluorobenzyl esterification of a carboxylic acid introduces a net increase of 180 Da. Methoxime and pentafluorobenzyl derivatives of pure OxPAFs obtained by chemical synthesis were also prepared as authentic standards. Each derivative was purified using a C18 minicolumn and then subject to LC-ESI-MS/MS analyses in positive mode.

Representative MRM chromatographs are shown in **Figs. 6–8**. The predicted ions for methoxime derivatives of OB-PAF (*m/z* 595), HOHA-PAF (*m/z* 651), KHdiA-PAF (*m/z* 665), OV-PAF (*m/z* 609), HOOA-PAF (*m/z* 665), KOdiA-PAF (*m/z* 679), ON-PAF (*m/z* 665), HODA-PAF

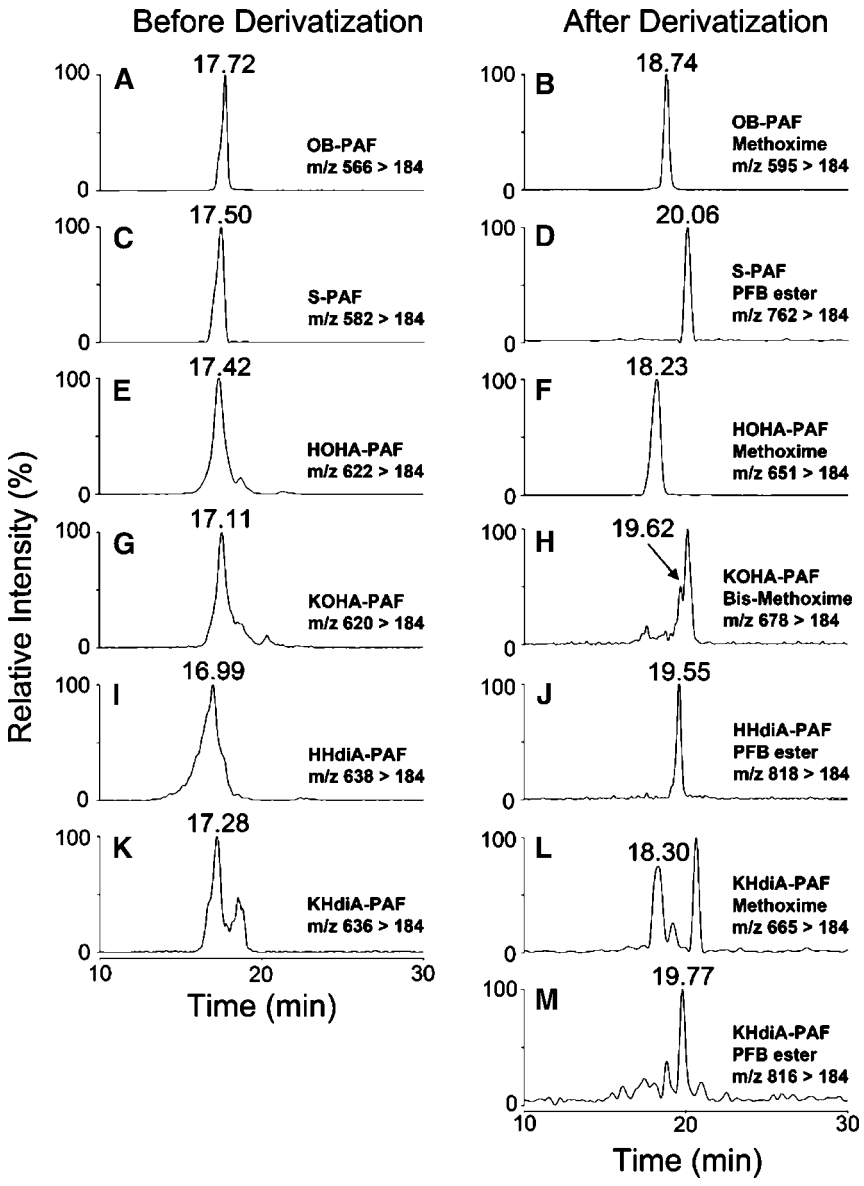

Fig. 6. LC-ESI-MS/MS analysis of lipid products from DHA-PAF oxidation in the presence of the MPO/H_2O_2/NO_2^- system. A: OB-PAF, multiple reaction monitoring (MRM) chromatogram (566 > 184). B: OB-PAF methoxime, MRM chromatogram (595 > 184). C: S-PAF, MRM chromatogram (582 > 184). D: S-PAF pentafluorobenzyl ester, MRM chromatogram (762 > 184). E: HOHA-PAF, MRM chromatogram (622 > 184). F: HOHA-PAF methoxime, MRM chromatogram (651 > 184). G: KOHA-PAF, MRM chromatogram (620 > 184). H: KOHA-PAF bis-methoxime, MRM chromatogram (678 > 184). I: HHdiA-PAF, MRM chromatogram (638 > 184). J: HHdiA-PAF pentafluorobenzyl ester, MRM chromatogram (818 > 184). K: KHdiA-PAF, MRM chromatogram (636 > 184). L: KHdiA-PAF methoxime, MRM chromatogram (665 > 184). M: KHdiA-PAF pentafluorobenzyl ester, MRM chromatogram (816 > 184).

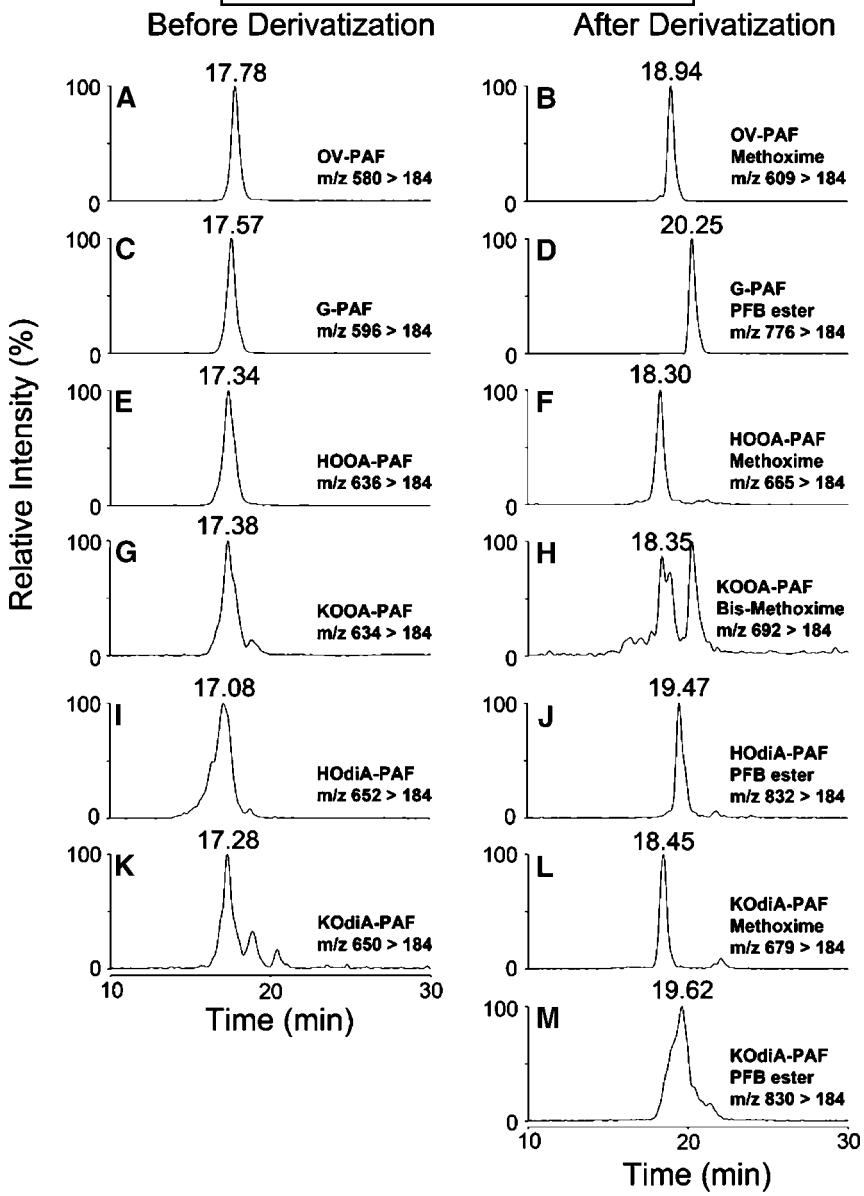

Fig. 7. LC-ESI-MS/MS analysis of lipid products from AA-PAF oxidation in the presence of the MPO/H_2O_2/NO_2^- system. A: OV-PAF, MRM chromatogram (580 > 184). B: OV-PAF methoxime, MRM chromatogram (609 > 184). C: G-PAF, MRM chromatogram (596 > 184). D: G-PAF pentafluorobenzyl ester, MRM chromatogram (776 > 184). E: HOOA-PAF, MRM chromatogram (636 > 184). F: HOOA-PAF methoxime, MRM chromatogram (665 > 184). G: KOOA-PAF, MRM chromatogram (634 > 184). H: KOOA-PAF bis-methoxime, MRM chromatogram (692 > 184). I: HOdiA-PAF, MRM chromatogram (652 > 184). J: HOdiA-PAF pentafluorobenzyl ester, MRM chromatogram (832 > 184). K: KOdiA-PAF, MRM chromatogram (650 > 184). L: KOdiA-PAF methoxime, MRM chromatogram (679 > 184). M: KOdiA-PAF pentafluorobenzyl ester, MRM chromatogram (830 > 184).

(*m/z* 721), and KDdiA-PAF (*m/z* 735) are consistent with the addition of a methoxime group (29 Da) to OB-PAF (*m/z* 566), HOHA-PAF (*m/z* 622), OV-PAF (*m/z* 580), HOOA-PAF (*m/z* 636), ON-PAF (*m/z* 636), and HODA-PAF (*m/z* 692). The derivatization of KOHA-PAF (*m/z* 620), KOOA-PAF (*m/z* 634), and KODA-PAF (*m/z* 690) was expected to introduce two methoxime groups (58 Da) to the respective lipid because of the derivatization of two carbonyl groups. Pentafluorobenzyl derivatization of S-PAF (*m/z* 582), KHdiA-PAF (*m/z* 636), HHdiA-PAF (*m/z* 638), G-PAF (*m/z* 596), KOdiA-PAF (*m/z* 650), HOdiA-PAF (*m/z* 652), A-PAF (*m/z* 652), KDdiA-PAF (*m/z* 706), and HDdiA-PAF (*m/z* 708) resulted in a net increase of 180 Da in derivatives. Thus, the expected mass increases were observed for all of the products of derivatization. The identities of the derivatives were also confirmed by their retention times, which were identical to those of the corresponding authentic standards.

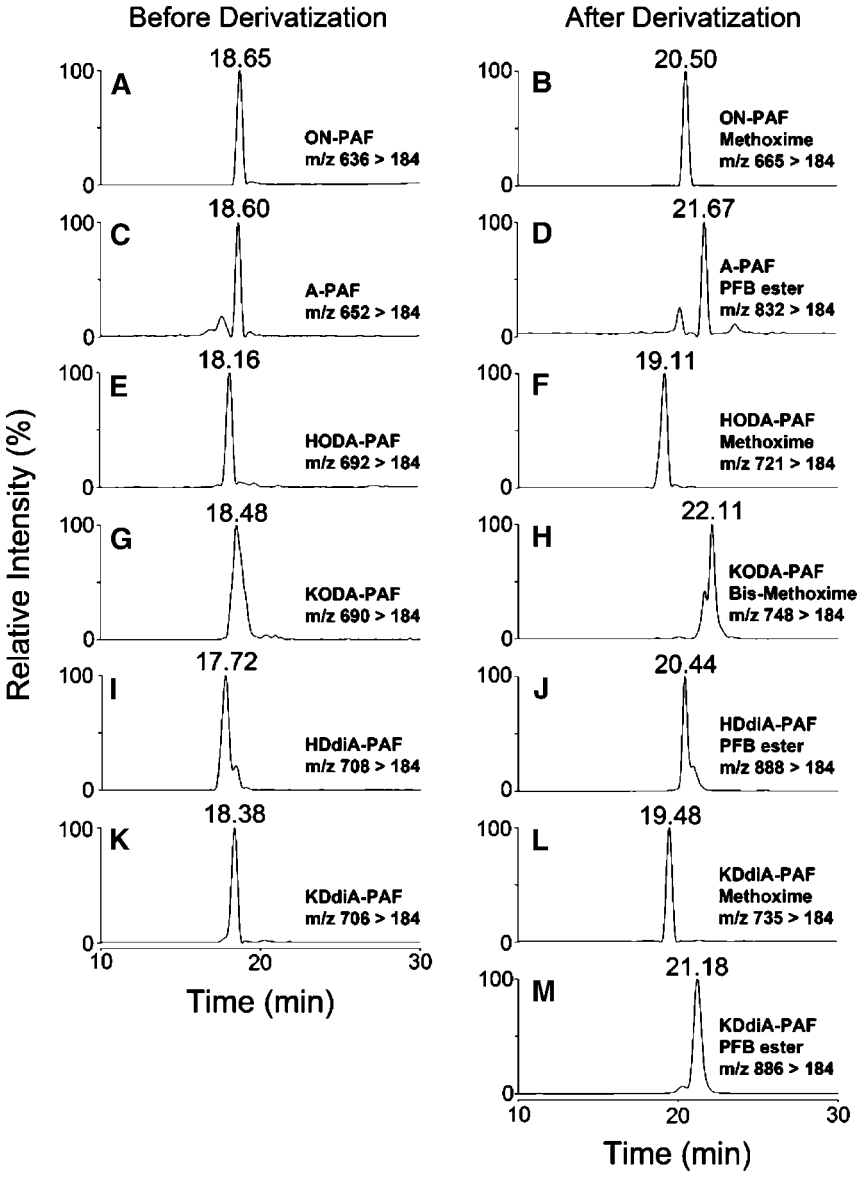

Fig. 8. LC-ESI-MS/MS analysis of lipid products from LA-PAF oxidation in the presence of the MPO/H_2O_2/NO_2^- system. A: ON-PAF, MRM chromatogram (636 > 184). B: ON-PAF methoxime, MRM chromatogram (665 > 184). C: A-PAF, MRM chromatogram (652 > 184). D: A-PAF pentafluorobenzyl ester, MRM chromatogram (832 > 184). E: HODA-PAF, MRM chromatogram (692 > 184). F: HODA-PAF methoxime, MRM chromatogram (721 > 184). G: KODA-PAF, MRM chromatogram (690 > 184). H: KODA-PAF bis-methoxime, MRM chromatogram (748 > 184). I: HDdiA-PAF, MRM chromatogram (708 > 184). J: HDdiA-PAF pentafluorobenzyl ester, MRM chromatogram (888 > 184). K: KDdiA-PAF, MRM chromatogram (706 > 184). L: KDdiA-PAF methoxime, MRM chromatogram (735 > 184). M: KDdiA-PAF pentafluorobenzyl ester, MRM chromatogram (886 > 184).

In saturated fatty acyl SUVs, HOHA-PAF resists further oxidative fragmentation

The generation of oxidatively truncated phospholipids, such as HOHA-PC or HOHA-PAF, containing γ-hydroxyalkenal functionality is of special interest. The γ-hydroxyalkenal OxPCs are ligands for the scavenger receptor CD36, a biological activity that they share with their more oxidized cousins (e.g., KOHA-PC, HHdiA-PC, and KHdiA-PC). OxPCs that bind strongly with this receptor, $OxPC_{CD36}$, possess a γ-hydroxy (or oxo) α,β-unsaturated carbonyl array. Binding of $OxPC_{CD36}$ with this receptor promotes the endocytosis of OxLDL (16, 28) and apoptotic cells (36) by macrophages and of oxidatively damaged photoreceptor rod outer segments by retinal pigmented endothelial cells (17). Furthermore, OxPCs containing γ-hydroxyalkenal functionality covalently modify proteins. Such modification inhibits the enzymatic activity or post-translational processing required to generate biologically active forms from inactive precursor proteins (20). HOHA-PC-derived protein modifications are biologically active. Thus, the reaction of HOHA-PCs with proteins generates CEP derivatives (26) (**Fig. 9**) that accumulate in the retinas

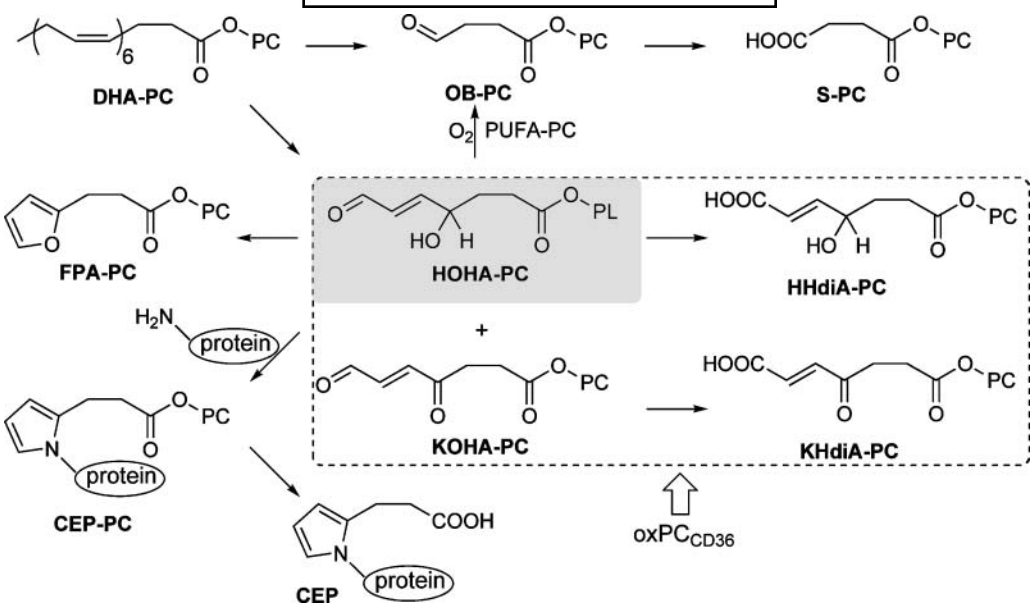

Fig. 9. Formation, transformations, and protein adduction of HOHA-PAF. CEP, carboxyethylpyrrole; FPA, 3-(2-furyl)propionic acid; PC, phosphatidylcholine.

of individuals with age-related macular degeneration (37, 38). CEP-modified proteins promote angiogenesis, leading to choroidal neovascularization in the retina, a pathological development that is associated with the advanced stages of age-related macular degeneration (21).

In view of the unique biological involvements of γ-hydroxyalkenal OxPCs, such as HOHA-PC, and the potential for these and other activities of the analogous γ-hydroxyalkenal OxPAFs, it is important to understand the reactions that consume them. We recently showed that spontaneous conversion into furans [e.g., the formation of a 3-(2-furyl)propionyl derivatives 1-palmityl-2-(3-(2-furyl)propionyl)-*sn*-glycero-3-phosphatidylcholines from HOHA-PCs] (Fig. 9) abolishes recognition by CD_{36} (39). To test the proclivity of HOHA-PAF toward further oxidative modification, we exposed liposomes containing 10% HOHA-PAF in a saturated diacylphosphatidylcholine carrier to the MPO/H_2O_2/NO_2^- system. At the indicated times, lipid products were extracted by the Bligh and Dyer method (29). The reaction product mixture was analyzed by LC-MS/MS. By qualitative and quantitative comparisons with the corresponding pure authentic samples that were available from unambiguous total syntheses, the further oxidative modification of HOHA-PAF was monitored. Quantification of the OxPAFs was achieved using MRM. 1-*O*-Hexadecyl-2-tridecanoyl-*sn*-glycero-3-phosphatidylcholine was added to the reaction mixture before the Bligh and Dyer (29) extraction as an internal standard. The absolute amount of each compound was determined by integration of the peak area and comparison with that of the corresponding authentic standard of known concentration. With the exception of KOHA-PAF, only traces of other OxPAFs were generated (**Fig. 10**). However, this model system lacks an important component of the reaction mixtures generated during the autoxidation of polyunsaturated fatty acyl phospholipids (i.e., an autoxidizing polyunsaturated fatty acyl phospholipid).

Polyunsaturated phospholipids promote the oxidative fragmentation of HOHA-PAF in SUVs

We wondered whether the presence of polyunsaturated phospholipids in the reaction mixture might influence the proclivity of HOHA-PAF toward further oxidative modification. Therefore, we exposed liposomes containing a 1:1 mixture of HOHA-PAF and LA-PC to the MPO/H_2O_2/NO_2^- system, extracting and analyzing the products as described above for liposomes not containing the polyunsaturated diacyl-PC. Figure 10 and **Table 4** show the time course and yield for OxPAFs generated upon the oxidation of HOHA-PAF promoted by MPO, both with or without the presence of LA-PC. As shown in Fig. 10A and Table 4, further oxidative fragmentation of HOHA-PAF to give OB-PAF occurred under both conditions. However, in the presence of LA-PC, the production of OB-PAF increased quickly during the first 10 h and subsequently slowed, and the yield of OB-PAF after 25 h reached 0.24%. This is four times more than the yield (0.06%) in the absence of LA-PC. Production of S-PAF displayed an almost linear increase with time when LA-PC was included in the reaction system. After 25 h in the presence of LA-PC, the yield of S-PAF reached 0.98%, but it was only 0.30% in the absence of LA-PC. Also, as shown in Fig. 10B and Table 4, the production of KOHA-PAF increased continually in the presence of LA-PC, reaching a maximum yield (5.5%) in the first 10 h and then decreasing to 3.7% yield after 25 h. This decrease can be explained by the presumption that LA-PC promotes the further oxidative modification of KOHA-PAF. In contrast, in the absence of LA-PC, the generation of KOHA-PAF was ini-

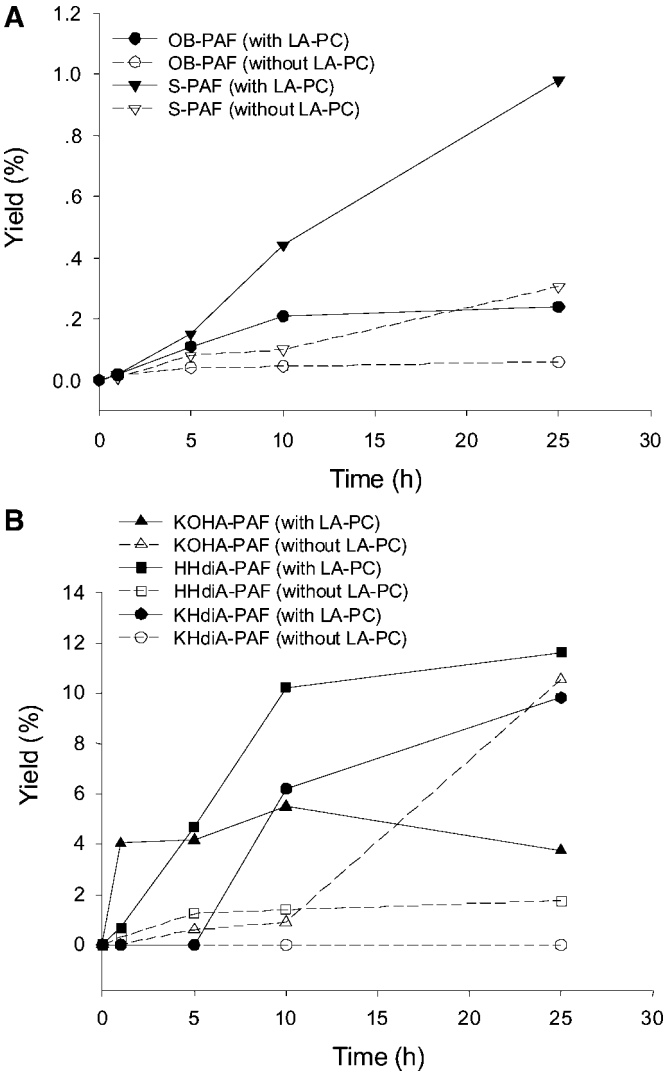

Fig. 10. Evolution profiles of the generation of OB-PAF and S-PAF with or without the presence of the linoleic acid ester of 2-lysophosphatidylcholine (LA-PC) (A) and the generation of KOHA-PAF, KHdiA-PAF, and HHdiA-PAF with or without the presence of LA-PC (B). Data are averages of three sets of independent experiments.

tially slow, but the yield continued to increase over time. The evolution profile of KHdiA-PAF supports this explanation. As the product of further oxidation of KOHA-PAF, KHdiA-PAF was not observed in the first 5 h when LA-PC was included in the reaction system. After that, the generation of KHdiA-PAF was detected, reaching a 9.8% maximum yield. There was no KHdiA-PAF generated in the absence of LA-PC. Compared with KHdiA-PAF, more HHdiA-PAF was produced from its precursor HOHA-PAF. The maximum yields were 11.6% with the presence of LA-PC but only 1.8% without the presence of LA-PC. As shown in Table 4, ~80% HOHA-PAF was consumed after 25 h in the presence of LA-PC but only 65% was consumed in the absence of LA-PC.

A likely mechanism for the effects of LA-PC on the oxidative fragmentation of HOHA-PAF to OB-PAF and S-PAF is presented in **Fig. 11**. Abstraction of a bisallylic hydrogen atom in the *sn*-2 side chain of LA-PC results in a pentadienyl radical that reacts with molecular oxygen to give peroxy radicals, LOO• (Fig. 11, left side). Addition of these peroxy radicals to the conjugated C=C bond in HOHA-PAF generates intermediate β-hydroxyperoxides (Fig. 11, right side). Subsequent fragmentation of the β-hydroxyperoxides (40) generates OB-PAF, malondialdehyde, and hydroxylipids. This fragmentation is driven by the simultaneous generation of two carbon-oxygen π bonds, one in OB-PAF and one in malondialdehyde, at the expense of weaker C-C and O-O σ bonds. In the absence of LA-PC, small quantities of acylperoxy radicals, generated during the autoxidation of aldehydes, can replace the can replace the peroxyoctadecadienoyl phosphatidylcholines represented by LOO• in this scheme.

Conversion of HOHA-PAF into HHdiA-PAF and KHdiA-PAF is promoted by cooxidation with polyunsaturated phospholipids

As noted above, HOHA-PCs are both ligands for the scavenger receptor CD36 and reactive molecules that transform proteins into biologically active CEP derivatives. The data in Fig. 10 show that cooxidation of a HOHA-PAF with the polyunsaturated phospholipid LA-PC not only generates a shorter chain stable end product, S-PAF, but also strongly promotes the formation of stable products that retain the functional motif of $OxPC_{CD36}$ (i.e., KHdiA-PAF and HHdiA-PAF), and these are the primary end products generated from HOHA-PAF. The ability of LA-PC to foster the formation of these products undoubtedly arises from the production of lipid-derived radicals from LA-PC (i.e., LO• and LOO•) that can abstract allylic or aldehydic hydrogen atoms (Fig. 11). Reaction of the resulting allylic and acyl radicals with oxygen ultimately delivers PAFs containing HHdiA and KHdiA.

TABLE 4. The yield of OxPAFs from the oxidation of HOHA-PAF in the presence or absence of LA-PC

	OB-PAF		S-PAF		KOHA-PAF		KHdiA-PAF		HHdiA-PAF		HOHA-PAF	
Time (h)	w	w/o	w	w/o	w	w/o	w	w/o	w	w/o	w	w/o
0	0.00	0.00	0.00	0.00	0.00	0.00	0.00	0.00	0.00	0.00	100.00	100.00
1	0.02	0.01	0.02	0.01	4.04	0.02	0.00	0.00	0.67	0.30	99.47	91.98
5	0.11	0.04	0.15	0.08	4.16	0.60	0.00	0.00	4.70	1.25	77.97	79.55
10	0.21	0.04	0.44	0.10	5.50	0.90	6.19	0.00	10.23	1.40	51.77	64.44
25	0.24	0.06	0.98	0.30	3.74	10.56	9.82	0.00	11.62	1.75	19.08	35.74

LA-PC, linoleic acid ester of 2-lysophosphatidylcholine. Each value is the average of three independent studies (n = 3). w indicates the presence of LA-PC, and w/o indicates the absence of LA-PC.

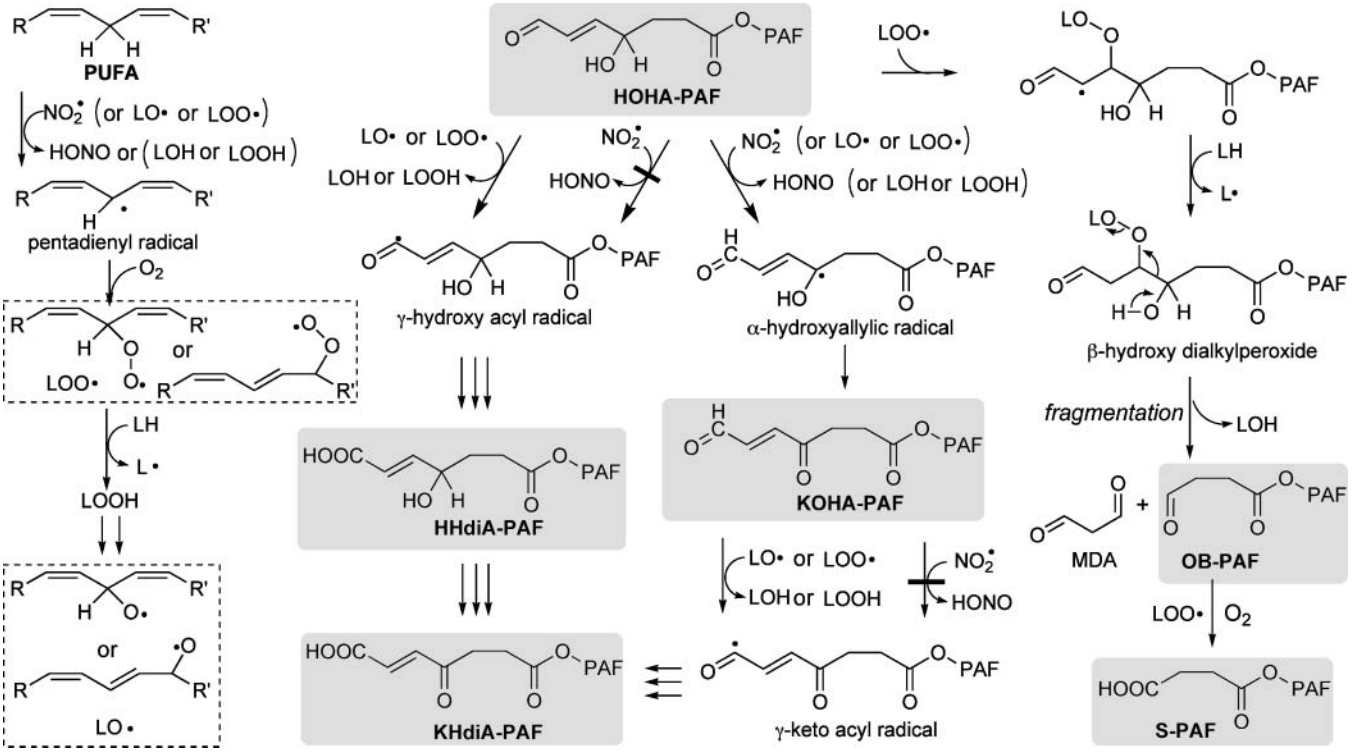

Fig. 11. Proposed mechanisms for the fragmentation of HOHA-PAF and the oxidative conversion of HOHA-PAF into HHdiA-PAF and KHdiA-PAF, which are promoted by polyunsaturated phospholipids (LH). LO• and LOO• are alkoxy and alkylperoxy radicals derived by hydrogen abstraction from LH. This mechanistic scheme also accounts for similar reactions of diacyl phospholipid analogs such as HOHA-PC and HOHA-PE. LOH, hydroxylipid; MDA, malondialdehyde.

Apparently, the $\bullet NO_2$ generated by MPO is reactive enough to abstract a hydrogen atom α to an allylic hydroxyl to produce a ketone (e.g., KOHA-PAF) but is not reactive enough to readily abstract an aldehydic hydrogen atom to produce carboxylic acids (e.g., HHdiA-PAF, KHdiA-PAF, or S-PAF) (Fig. 11). In contrast, peroxy or alkoxy radicals, generated during the autoxidation of polyunsaturated lipids, are more reactive and can convert aldehyde groups into carboxylic acids as well as induce the oxidative cleavage of γ-hydroxyalkenals. This important role of PUFA-derived peroxy or alkoxy radicals in fostering the oxidation of lipid-derived aldehydes to carboxylic acids has not been recognized previously.

Biological consequences of the generation of OxPAF and of the remarkable influence of a saturated versus a polyunsaturated membrane environment on the lifetime (stability) of γ-hydroxyalkenals

Although ether phospholipids are only minor components of LDL, in view of the exceptional activity of PAF, OxPAFs may have biological significance that is much greater than their relative abundance. The pure samples of OxPAFs that are now available through the chemical syntheses reported above not only were valuable for confirming the identities of OxPAFs generated upon the autoxidation of polyunsaturated esters of 2-lyso-PAF but also will facilitate their detection and quantification in biological samples and the evaluation of their biological activities.

In view of the profound influence of polyunsaturated lipids on the stability (lifetime), the percent polyunsaturated composition of membrane lipids is an important factor in determining the biological sequelae of the generation of these products of oxidative lipid fragmentation. The percent polyunsaturated composition of membrane lipids varies widely (see supplementary Table I), and for some tissues only the composition of specific classes of phospholipids, and not the composition of all phospholipids, has been determined. Further complexity is engendered by inhomogeneities in the local distribution of lipids within membranes. In particular, membrane lipids are laterally segregated into PUFA-rich regions and PUFA-poor rafts (41) whose polar lipids contain predominantly saturated fatty acyl chains (42). Thus, it is expected that γ-hydroxyalkenals would be protected in lipid rafts against conversion into the corresponding carboxylic acids. Consequently, raft-associated proteins should be especially susceptible to covalent modification by these and other aldehydic products of oxidative lipid fragmentation. Similarly, covalent modification by lipid-derived aldehydes is expected for proteins in tissues with a globally low content of PUFAs (e.g., 14% in brain white matter). This may contribute to the occurrence of lipid-derived protein modifications in the brain. Thus, we recently reported that, remarkably, localized CEP and iso[4]levuglandin E_2-derived protein modifications, which appear as filaments in the cortical tissue, are a hallmark of the autistic brain (43). Of course, a low level of PUFAs can also result in little or no

susceptibility to oxidative damage, as PUFAs are the targets of free radical-induced lipid oxidation. Large surfactant aggregates present in bronchoaveolar lavage fluid contain only 3% of PUFAs (44). Low oxidizability is almost certainly a biologically important role of the disaturated PC (surfactant) present in the lung, a tissue that is exposed to exceptionally high oxygen tension.

It should be noted that the presence of polyunsaturated PCs in the membrane, modeled with SUVs, militates against the production of HOHA-derived CEP protein modifications (Fig. 9) and consequent biological responses (e.g., angiogenesis). But the predominant further oxidative modification of phospholipids containing HOHA (e.g., HOHA-PAF, HOHA-PC, or HOHA-PE), which is promoted by polyunsaturated PCs, not only does not abolish their potential as ligands for the scavenger receptor CD36 but converts them to chemically stable end products. Thus, although the high DHA content of photoreceptor disk membranes and the high level of PUFAs (49%) make them highly susceptible to free radical-induced oxidative fragmentation (e.g., to HOHA derivatives), it also militates against the formation of pathological CEP protein modifications by promoting the destruction of HOHA derivatives through further oxidative fragmentation and oxidation to ligands that promote their CD36-mediated clearance (e.g., KHdiA derivatives). In view of these considerations, it is all the more remarkable that grossly increased levels of CEP-modified proteins are present in the retinal rod outer segments and retinal pigmented epithelial cells of individuals with age-related macular degeneration (37). Thus, the low levels of these modifications present in healthy eyes are the expected consequence of the efficient clearance of HOHA derivatives through PUFA-promoted oxidation. Available online are ^{1}H and ^{13}C NMR spectra for all new compounds, a microphosphorous assay calibration curve, and a table presenting the percent polyunsaturated lipids in various human tissues.

The authors thank the National Institutes of Health for support of this research by Grants GM-21249 (R.G.S.), HL-53315 (R.G.S.), EY-016813 (R.G.S.), HL-087018 (R.G.S. and S.L.H.), HL-70621 (S.L.H.), P01 HL-076491 (S.L.H.), and P01 HL-077107 (S.L.H.).

REFERENCES

1. Ross, R. 1995. Cell biology of atherosclerosis. *Annu. Rev. Physiol.* **57:** 791–804.
2. Hoff, H. F., C. L. Heideman, J. W. Gaubatz, A. M. Gotto, Jr., E. E. Erickson, and R. L. Jackson. 1977. Quantification of apolipoprotein B in grossly normal human aorta. *Circ. Res.* **40:** 56–64.
3. Steinberg, D., S. Parthasarathy, T. E. Carew, J. C. Khoo, and J. L. Witztum. 1989. Beyond cholesterol. Modifications of low-density lipoprotein that increase its atherogenicity. *N. Engl. J. Med.* **320:** 915–924.
4. Witztum, J. L., and D. Steinberg. 1991. Role of oxidized low density lipoprotein in atherogenesis. *J. Clin. Invest.* **88:** 1785–1792.
5. Henriksen, T., E. M. Mahoney, and D. Steinberg. 1981. Enhanced macrophage degradation of low density lipoprotein previously incubated with cultured endothelial cells: recognition by receptors for acetylated low density lipoproteins. *Proc. Natl. Acad. Sci. USA.* **78:** 6499–6503.
6. Steinberg, D. 1997. Low density lipoprotein oxidation and its pathobiological significance. *J. Biol. Chem.* **272:** 20963–20966.
7. Tokumura, A., M. Toujima, Y. Yoshioka, and K. Fukuzawa. 1996. Lipid peroxidation in low density lipoproteins from human plasma and egg yolk promotes accumulation of 1-acyl analogues of platelet-activating factor-like lipids. *Lipids.* **31:** 1251–1258.
8. Heery, J. M., M. Kozak, D. M. Stafforini, D. A. Jones, G. A. Zimmerman, T. M. McIntyre, and S. M. Prescott. 1995. Oxidatively modified LDL contains phospholipids with platelet-activating factor-like activity and stimulates the growth of smooth muscle cells. *J. Clin. Invest.* **96:** 2322–2330.
9. Marathe, G. K., S. S. Davies, K. A. Harrison, A. R. Silva, R. C. Murphy, H. Castro-Faria-Neto, S. M. Prescott, G. A. Zimmerman, and T. M. McIntyre. 1999. Inflammatory platelet-activating factor-like phospholipids in oxidized low density lipoproteins are fragmented alkyl phosphatidylcholines. *J. Biol. Chem.* **274:** 28395–28404.
10. Berliner, J. A., G. Subbanagounder, N. Leitinger, A. D. Watson, and D. Vora. 2001. Evidence for a role of phospholipid oxidation products in atherogenesis. *Trends Cardiovasc. Med.* **11:** 142–147.
11. Watson, A. D., N. Leitinger, M. Navab, K. F. Faull, S. Horkko, J. L. Witztum, W. Palinski, D. Schwenke, R. G. Salomon, W. Sha, et al. 1997. Structural identification by mass spectrometry of oxidized phospholipids in minimally oxidized low density lipoprotein that induce monocyte/endothelial interactions and evidence for their presence in vivo. *J. Biol. Chem.* **272:** 13597–13607.
12. Watson, A. D., M. Navab, S. Y. Hama, A. Sevanian, S. M. Prescott, D. M. Stafforini, T. M. McIntyre, B. N. Du, A. M. Fogelman, and J. A. Berliner. 1995. Effect of platelet activating factor-acetylhydrolase on the formation and action of minimally oxidized low density lipoprotein. *J. Clin. Invest.* **95:** 774–782.
13. Parhami, F., A. D. Morrow, J. Balucan, N. Leitinger, A. D. Watson, Y. Tintut, J. A. Berliner, and L. L. Demer. 1997. Lipid oxidation products have opposite effects on calcifying vascular cell and bone cell differentiation. A possible explanation for the paradox of arterial calcification in osteoporotic patients. *Arterioscler. Thromb. Vasc. Biol.* **17:** 680–687.
14. Subbanagounder, G., Y. Deng, C. Borromeo, A. N. Dooley, J. A. Berliner, and R. G. Salomon. 2002. Hydroxy alkenal phospholipids regulate inflammatory functions of endothelial cells. *Vascul. Pharmacol.* **38:** 201–209.
15. Podrez, E. A., M. Febbraio, N. Sheibani, D. Schmitt, R. L. Silverstein, D. P. Hajjar, P. A. Cohen, W. A. Frazier, H. F. Hoff, and S. L. Hazen. 2000. Macrophage scavenger receptor CD36 is the major receptor for LDL modified by monocyte-generated reactive nitrogen species. *J. Clin. Invest.* **105:** 1095–1108.
16. Podrez, E. A., E. Poliakov, Z. Shen, R. Zhang, Y. Deng, M. Sun, P. J. Finton, L. Shan, B. Gugiu, P. L. Fox, et al. 2002. Identification of a novel family of oxidized phospholipids that serve as ligands for the macrophage scavenger receptor CD36. *J. Biol. Chem.* **277:** 38503–38516.
17. Sun, M., S. C. Finnemann, M. Febbraio, L. Shan, S. P. Annangudi, E. A. Podrez, G. Hoppe, R. Darrow, D. T. Organisciak, R. G. Salomon, et al. 2006. Light-induced oxidation of photoreceptor outer segment phospholipids generates ligands for CD36-mediated phagocytosis by retinal pigment epithelium: a potential mechanism for modulating outer segment phagocytosis under oxidant stress conditions. *J. Biol. Chem.* **281:** 4222–4230.
18. Boullier, A., K. L. Gillotte, S. Horkko, S. R. Green, P. Friedman, E. A. Dennis, J. L. Witztum, D. Steinberg, and O. Quehenberger. 2000. The binding of oxidized low density lipoprotein to mouse CD36 is mediated in part by oxidized phospholipids that are associated with both the lipid and protein moieties of the lipoprotein. *J. Biol. Chem.* **275:** 9163–9169.
19. Karakatsani, A. I., T. A. Liapikos, A. N. Troganis, and D. C. Tsoukatos. 1998. Involvement of phospholipids in apolipoprotein B modification during low density lipoprotein oxidation. *Lipids.* **33:** 1159–1162.
20. Hoff, H. F., J. O'Neil, Z. Wu, G. Hoppe, and R. L. Salomon. 2003. Phospholipid hydroxyalkenals: biological and chemical properties of specific oxidized lipids present in atherosclerotic lesions. *Arterioscler. Thromb. Vasc. Biol.* **23:** 275–282.
21. Ebrahem, Q., K. Renganathan, J. Sears, A. Vasanji, X. Gu, L. Lu, R. G. Salomon, J. W. Crabb, and B. Anand-Apte. 2006. Carboxyethylpyrrole oxidative protein modifications stimulate neovascu-

larization: implications for age-related macular degeneration. *Proc. Natl. Acad. Sci. USA.* **103:** 13480–13484.
22. Prescott, S. M., G. A. Zimmerman, D. M. Stafforini, and T. M. McIntyre. 2000. Platelet-activating factor and related lipid mediators. *Annu. Rev. Biochem.* **69:** 419–445.
23. Ishii, S., and T. Shimizu. 2000. Platelet-activating factor (PAF) receptor and genetically engineered PAF receptor mutant mice. *Prog. Lipid Res.* **39:** 41–82.
24. Marathe, G. K., K. A. Harrison, R. C. Murphy, S. M. Prescott, G. A. Zimmerman, and T. M. McIntyre. 2000. Bioactive phospholipid oxidation products. *Free Radic. Biol. Med.* **28:** 1762–1770.
25. Davies, S. S., A. V. Pontsler, G. K. Marathe, K. A. Harrison, R. C. Murphy, J. C. Hinshaw, G. D. Prestwich, A. S. Hilaire, S. M. Prescott, G. A. Zimmerman, et al. 2001. Oxidized alkyl phospholipids are specific, high affinity peroxisome proliferator-activated receptor gamma ligands and agonists. *J. Biol. Chem.* **276:** 16015–16023.
26. Gu, X., M. Sun, B. Gugiu, S. Hazen, J. W. Crabb, and R. G. Salomon. 2003. Oxidatively truncated docosahexaenoate phospholipids: total synthesis, generation, and peptide adduction chemistry. *J. Org. Chem.* **68:** 3749–3761.
27. Gugiu, B. G., C. A. Mesaros, M. Sun, X. Gu, J. W. Crabb, and R. G. Salomon. 2006. Identification of oxidatively truncated ethanolamine phospholipids in retina and their generation from polyunsaturated phosphatidylethanolamines. *Chem. Res. Toxicol.* **19:** 262–271.
28. Podrez, E. A., E. Poliakov, Z. Shen, R. Zhang, Y. Deng, M. Sun, P. J. Finton, L. Shan, M. Febbraio, D. P. Hajjar, et al. 2002. A novel family of atherogenic oxidized phospholipids promotes macrophage foam cell formation via the scavenger receptor CD36 and is enriched in atherosclerotic lesions. *J. Biol. Chem.* **277:** 38517–38523.
29. Bligh, E. G., and W. J. Dyer. 1959. A rapid method of total lipid extraction and purification. *Can. J. Biochem. Physiol.* **37:** 911–917.
30. Kates, M. 1986. Techniques of Lipidology: Isolation, Analysis and Identification of Lipids. 2nd revised edition. (Elsevier, Amsterdam).
31. Deng, Y., and R. G. Salomon. 1998. Synthesis of [9-^{3}H]-trans-4-hydroxy-2-nonenal. *J. Org. Chem.* **63:** 3504–3507.
32. Sun, M., Y. Deng, E. Batyreva, W. Sha, and R. G. Salomon. 2002. Novel bioactive phospholipids: practical total syntheses of products from the oxidation of arachidonic and linoleic esters of 2-lysophosphatidylcholine(1). *J. Org. Chem.* **67:** 3575–3584.
33. Hazen, S. L., R. Zhang, Z. Shen, W. Wu, E. A. Podrez, J. C. MacPherson, D. Schmitt, S. N. Mitra, C. Mukhopadhyay, Y. Chen, et al. 1999. Formation of nitric oxide-derived oxidants by myeloperoxidase in monocytes: pathways for monocyte-mediated protein nitration and lipid peroxidation in vivo. *Circ. Res.* **85:** 950–958.
34. Noguchi, N., K. Nakano, Y. Aratani, H. Koyama, T. Kodama, and E. Niki. 2000. Role of myeloperoxidase in the neutrophil-induced oxidation of low density lipoprotein as studied by myeloperoxidase-knockout mouse. *J. Biochem. (Tokyo).* **127:** 971–976.
35. van der Vliet, A., J. P. Eiserich, B. Halliwell, and C. E. Cross. 1997. Formation of reactive nitrogen species during peroxidase-catalyzed oxidation of nitrite. A potential additional mechanism of nitric oxide-dependent toxicity. *J. Biol. Chem.* **272:** 7617–7625.
36. Greenberg, M. E., M. Sun, R. Zhang, M. Febbraio, R. Silverstein, and S. L. Hazen. 2006. Oxidized phosphatidylserine-CD36 interactions play an essential role in macrophage-dependent phagocytosis of apoptotic cells. *J. Exp. Med.* **203:** 2613–2625.
37. Gu, X., S. G. Meer, M. Miyagi, M. E. Rayborn, J. G. Hollyfield, J. W. Crabb, and R. G. Salomon. 2003. Carboxyethylpyrrole protein adducts and autoantibodies, biomarkers for age-related macular degeneration. *J. Biol. Chem.* **278:** 42027–42035.
38. Crabb, J. W., M. Miyagi, X. Gu, K. Shadrach, K. A. West, H. Sakaguchi, M. Kamei, A. Hasan, L. Yan, M. E. Rayborn, et al. 2002. Drusen proteome analysis: an approach to the etiology of age-related macular degeneration. *Proc. Natl. Acad. Sci. USA.* **99:** 14682–14687.
39. Gao, S., R. Zhang, M. E. Greenberg, M. Sun, X. Chen, B. S. Levison, R. G. Salomon, and S. L. Hazen. 2006. Phospholipid hydroxyalkenals, a subset of recently discovered endogenous CD36 ligands, spontaneously generate novel furan-containing phospholipids lacking CD36 binding activity in vivo. *J. Biol. Chem.* **281:** 31298–31308.
40. Balamraju, Y. N., M. Sun, and R. G. Salomon. 2004. Gamma-hydroxyalkenals are oxidatively cleaved through Michael addition of acylperoxy radicals and fragmentation of intermediate beta-hydroxyperesters. *J. Am. Chem. Soc.* **126:** 11522–11528.
41. Simons, K., and E. Ikonen. 1997. Functional rafts in cell membranes. *Nature.* **387:** 569–572.
42. Calder, P. C., and P. Yaqoob. 2007. Lipid rafts—composition, characterization, and controversies. *J. Nutr.* **137:** 545–547.
43. Evans, T. A., S. L. Siedlak, L. Lu, X. Fu, Z. Wang, W. R. McGinnis, E. Fakhoury, R. J. Castellani, S. L. Hazen, W. J. Walsh, et al. 2008. The autistic phenotype exhibits a remarkably localized modification of brain protein by products of free radical-induced lipid oxidation. *Am. J. Biotech. Biochem.* **4:** 61–72.
44. Schmidt, R., U. Meier, P. Markart, F. Grimminger, H. G. Velcovsky, H. Morr, W. Seeger, and A. Gunther. 2002. Altered fatty acid composition of lung surfactant phospholipids in interstitial lung disease. *Am. J. Physiol.* **283:** L1079–L1085.